Vertical Fluxes of Potential Vorticity and the Structure of the Thermocline

DAVID P. MARSHALL

Department of Meteorology, University of Reading, Reading, United Kingdom

(Manuscript received 16 March 1999, in final form 3 February 2000)

ABSTRACT

A new framework for understanding the vertical structure of ocean gyres is developed based on vertical fluxes of potential vorticity. The key ingredient is an integral constraint that in a steady state prohibits a net flux of potential vorticity through any closed contour of Bernoulli potential or density. Applied to an ocean gyre, the vertical fluxes of potential vorticity associated with advection, friction, and buoyancy forcing must therefore balance in an integral sense.

In an anticyclonic subtropical gyre, the advective and frictional potential vorticity fluxes are both directed downward, and buoyancy forcing is required to provide the compensating upward potential vorticity flux. Three regimes are identified: 1) a surface ''ventilated thermocline'' in which the upward potential vorticity flux is provided by buoyancy forcing within the surface mixed layer, 2) a region of weak stratification—''mode water''—in which all three components of the potential vorticity flux become vanishingly small, and 3) an ''internal boundary layer thermocline'' at the base of the gyre where the upward potential vorticity flux is provided by the diapycnal mixing. Within a cyclonic subpolar gyre, the advective and frictional potential vorticity fluxes are directed upward and downward, respectively, and are thus able to balance without buoyancy forcing.

Geostrophic eddies provide an additional vertical potential vorticity flux associated with slumping of isopycnals in baroclinic instability. Incorporating the eddy potential vorticity flux into the integral constraint provides insights into the role of eddies in maintaining the Antarctic Circumpolar Current and convective chimneys. The possible impact of eddies on the vertical structure of a wind-driven gyre is discussed.

1. Introduction

Since the seminal studies of Robinson and Stommel (1959) and Welander (1959), theories for the existence and structure of the subtropical thermocline have followed two distinct approaches. On the one hand, *internal boundary layer* thermocline theories (Robinson and Stommel 1959; Stommel and Webster 1962; Young and Ierley 1986; Salmon 1990) view the thermocline as an internal boundary layer, resulting from a balance between vertical advection and diffusion of density. In contrast, *ventilated* thermocline theories (Welander 1959, 1971; Luyten et al. 1983) view the thermocline as the result of the fluid parcels adiabatically advecting density variations from the sea surface downward into the gyre interior.

The debate over the relative merits of the two thermocline theories has recently been invigorated by Samelson and Vallis (1997). In an insightful series of numerical experiments, they demonstrate that *both* the internal boundary layer and ventilated thermoclines can form within a subtropical gyre. The upper thermocline forms at the base of the mixed layer and is well described by the ventilated theory, whereas the lower thermocline forms at the base of the gyre and is well described by the internal boundary layer theory. Sandwiched in between the two thermoclines is a region of low potential vorticity, reminiscent of the mode waters found in each of the subtropical basins (McCartney 1982).

A deficiency of both the internal boundary layer and ventilated thermocline theories is that neither is closed by a western boundary current. The validity of both theories thus relies on the implicit assumption that the western boundary current is passive, in the sense that it acts merely to close the circulation at the western boundary without modifying the properties of the Sverdrup interior. An analogous issue arises in the theory of the wind-driven circulation in a homogeneous ocean (e.g., Pedlosky 1996). There the dominant balance in the gyre interior is between advection of planetary vorticity and the source of vorticity by the wind stress curl (Sverdrup 1947). However, as demonstrated by Niiler (1966), the net sources and sinks of circulation along a streamline must always balance in a steady state. Even though friction is always small in the local vorticity balance, the circulation induced by the wind stress and dissipated by friction must balance along each stream-

Corresponding author address: Dr. David Marshall, Department of Meteorology, University of Reading, P.O. Box 243, Reading RG6 6BB, United Kingdom.
E-mail: davidm@met.reading.ac.uk

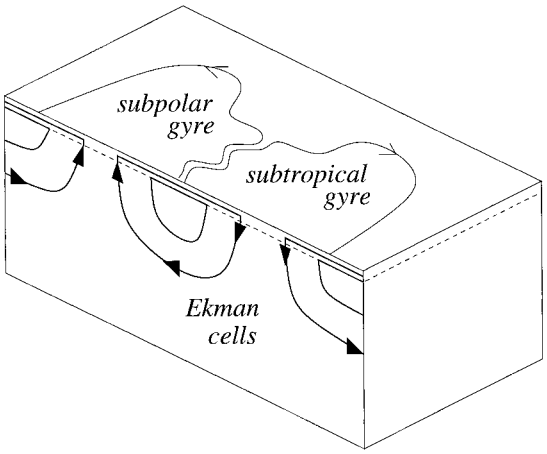

FIG. 1. A schematic diagram illustrating how water is pumped down from the surface Ekman layer in the subtropical gyre and upwells into the surface Ekman layer in the subpolar gyre. The buoyancy of the fluid parcels downwelling in the subtropical gyre is higher than the buoyancy of fluid parcels upwelling in the subpolar gyre, and thus fluid parcels must pass through a region of water mass transformation as they complete a circuit of the Ekman cell.

line. For realistic values of frictional coefficient, this condition is only achieved if the gyre transport increases above that predicted by Sverdrup balance, in a process termed ''inertial recirculation'' [see Pedlosky (1996) for a review].

The aim of this paper is to explore the hypothesis that the existence of two thermoclines and mode water can be understood through an analogous integral constraint that must be satisfied when a gyre is closed by a western boundary current. In this case the integral constraint acts on the vertical flux of potential vorticity within a gyre. The physical origin of constraint is illustrated in Fig. 1. To first approximation, fluid parcels circulate around closed geostrophic streamlines at a constant depth. However, superimposed on this geostrophic circulation is an ageostrophic ''Ekman cell''[1] connecting the subtropical gyre with the subpolar gyre to the north, and with the Tropics to the south (Fig. 1). Fluid parcels are pumped down from the surface Ekman layer into the subtropical gyre, are transported across geostrophic streamlines by the frictional Ekman velocity (or by eddies), and return back into the surface Ekman layer within the subpolar gyre or the Tropics. Since the buoyancy of the warm fluid pumped down into the subtropical gyre is higher than that of the cold fluid upwelling in the subpolar gyre, it is necessary to somehow transform the buoyancy of fluid parcels as they complete a circuit of the Ekman cell. It is this requirement for a region of water-mass transformation that leads to the establishment of an internal boundary layer thermocline at the base of the subtropical gyre.

The paper is structured in the following way. In section 2, the concept of potential vorticity flux vectors and the flux form of the potential vorticity equation are reviewed. By assuming a steady state, it is proved that net flux of potential vorticity through any closed contour of density or Bernoulli potential must vanish. Applied to the vertical flux of potential vorticity, the constraint provides an integral balance between vertical advection, buoyancy forcing, and mechanical forcing at each depth. In section 3, the implications of the integral constraint for the structure of a subtropical gyre are considered. It is argued that three regimes emerge: a surface ventilated thermocline, overlying a region of low potential vorticity mode water, in turn overlying an internal boundary layer thermocline. In section 4, an alternative physical interpretation is developed in terms of a buoyancy budget for the Ekman circulation within a gyre. In section 5, the integral constraint is extended to include the rectified effects of geostrophic eddies. Applications to the Antarctic Circumpolar Current and to buoyancy-driven gyres are presented, and the likely impact of eddies on subtropical gyres is conjectured. Section 6 contains a brief summary and discussion.

2. Potential vorticity fluxes and the integral constraint

We consider a continuously stratified ocean, exposed to arbitrary mechanical and buoyancy forcing. The equations of motion are written

$$\frac{\partial \mathbf{u}}{\partial t} + \mathbf{u}\cdot\nabla\mathbf{u} + 2\boldsymbol{\Omega}\times\mathbf{u} + \frac{\nabla p}{\rho_0} + \nabla\phi = \mathbf{F}, \quad (1)$$

$$\frac{\partial \rho}{\partial t} + \nabla\cdot(\rho\mathbf{u}) = 0, \quad (2)$$

$$\frac{\partial \rho}{\partial t} + \mathbf{u}\cdot\nabla\rho = \mathcal{B}, \quad (3)$$

where $\mathbf{u}$ is the three-dimensional fluid velocity, p is pressure, ρ is density, ρ_0 is a constant reference density,[2] ϕ is the gravitational potential, $\boldsymbol{\Omega}$ is the Earth's rotation vector, and $\mathbf{F}$ and $\mathcal{B}$ represent mechanical and buoyancy forcing (which may include the rectified effects of transients).

[1] Here the term ''Ekman cell'' refers to the wind-driven Ekman velocity within the surface Ekman layer, the downwelling and upwelling within the subtropical and subpolar gyres respectively, and the frictional Ekman velocity taking fluid parcels across geostrophic streamlines. A precise mathematical definition is given in section 4.

[2] To simplify the mathematical development, we invoke the Boussinesq approximation and also neglect the effects of compressibility in the equation of state. However it is possible to extend the results presented here to account for compressibility by writing (3) in terms of potential density (e.g., see Marshall et al. 2000).

a. Potential vorticity conservation and flux

Using (1)–(3), a conservation equation for the Ertel potential vorticity can be written in unapproximated flux form,

$$\frac{\partial}{\partial t}(\rho_0 Q) + \nabla \cdot \mathbf{J} = 0 \tag{4}$$

(Truesdell 1951; Obukhov 1962; Haynes and McIntyre 1987, 1990), where

$$Q = -\frac{\mathbf{q} \cdot \nabla \rho}{\rho_0} \tag{5}$$

is the Ertel potential vorticity and

$$\mathbf{q} = 2\boldsymbol{\Omega} + \nabla \times \mathbf{u}$$

is the absolute vorticity. The potential vorticity flux vector,

$$\mathbf{J} = \rho_0 Q\mathbf{u} + \mathbf{q}\mathcal{B} + \mathbf{F} \times \nabla \rho, \tag{6}$$

consists of three components involving advection, buoyancy forcing, and mechanical forcing. Physical illustrations of these components are given in McIntyre and Norton (1990). The flux form of the potential vorticity equation provides a powerful diagnostic tool for understanding the potential vorticity transport through an ocean gyre (Marshall and Nurser 1992; Marshall et al. 2000).

b. Impermeability theorem

A particularly useful property of the potential vorticity flux is embodied in an ''impermeability theorem'' derived by Haynes and McIntyre (1987). This states that isopycnals are impermeable to potential vorticity flux vectors. Changes in the potential vorticity within an isopycnal layer can therefore be understood purely in terms of concentration and dilution of the substance whose mixing ratio is potential vorticity (Haynes and McIntyre 1990). While this result is not central to the steady-state balances discussed in this paper, it is helpful in considering how the structure of the thermocline is established from an arbitrary initial state.

c. General integral constraint

We now assume a steady state, setting $\partial/\partial t = 0$ in Eqs. (1)–(3). The steady-state momentum equation (1) can be rewritten, using standard vector identities, in the form

$$\mathbf{q} \times \mathbf{u} + \nabla B = \mathbf{F}, \tag{7}$$

where

$$B = \frac{\mathbf{u} \cdot \mathbf{u}}{2} + \frac{p}{\rho_0} + \phi$$

is the Bernoulli potential. Taking the cross product of $\nabla\rho$ and (7) we obtain an alternative form for the potential vorticity flux vector,

$$\mathbf{J} = \nabla B \times \nabla \rho, \tag{8}$$

which thus lies along the intersection of surfaces of constant density and surfaces of constant Bernoulli potential (Schär 1993). Finally, integrating (8) over the area A enclosed by any contour of Bernoulli potential or density, using the vector identity

$$\nabla B \times \nabla \rho \equiv \nabla \times (B \nabla \rho) \equiv -\nabla \times (\rho \nabla B),$$

and invoking Stokes theorem, we obtain the integral constraint

$$\int_A \mathbf{J} \cdot d\mathbf{A} = 0. \tag{9}$$

In a steady state, the net potential vorticity flux through any closed contour of Bernoulli potential or density must therefore vanish.

d. Constraint on the vertical potential vorticity flux in a gyre

The integral constraint, (9), must be satisfied for *any* closed contour of Bernoulli potential or density. However for an ocean gyre, it is particularly helpful to focus on the *vertical* potential vorticity flux by applying the integral constraint over an area at constant depth. Thus choosing A to be the area enclosed by a contour of Bernoulli potential or density at an arbitrary depth z, we obtain:

$$\int_A (J_{\text{adv}} + J_{\text{buoy}} + J_{\text{fric}})\, dx\, dy = 0, \tag{10}$$

where

$$J_{\text{adv}} = \rho Q w, \tag{11}$$

$$J_{\text{buoy}} = q^{(z)}\mathcal{B}, \tag{12}$$

$$J_{\text{fric}} = -\mathbf{k} \times \nabla \rho \cdot \mathbf{F} \tag{13}$$

are the three components of the vertical potential vorticity flux associated with vertical advection, buoyancy forcing, and friction.

The integral balance (10) makes clear the important role of western boundary current in the vertical equilibration of ocean gyres. For example, in the ventilated thermocline theory of Luyten et al. (1983) the circulation is open at the western boundary, there are no closed Bernoulli or density contours, and thus there is no need to satisfy (10). However, once the circulation is closed at the western boundary, (10) *must* be satisfied and provides a strong constraint on the structure of the thermocline. Just as the net sources and sinks of circulation along any closed streamline must balance in a steady state (Niiler 1966), so the net vertical flux of

potential vorticity through any gyre must vanish in a steady state.

3. Application to a noneddying gyre

In this section, we discuss how the integral constraint (10) can help us understand the structure of the subtropical thermocline. Here we consider a steady-state gyre containing no transient eddies (a discussion of the effect of eddies is deferred until section 5). The approach taken is to first consider the adiabatic limit in which $\mathcal{B} \equiv 0$, and then add, in turn, finite diapycnal diffusion and a surface mixed layer of variable depth. For convenience the arguments are developed for a northern hemisphere.

a. Adiabatic limit

The simplest scenario one can consider is a completely adiabatic thermocline into which fluid is pumped from an overlying surface Ekman layer, as assumed in the ventilated thermocline model of Luyten et al. (1983). To proceed, it is necessary to make three further assumptions:

- There exist closed contours of density and/or Bernoulli potential at each depth along which one can apply the integral constraint (10). Inspection of the Lozier et al. (1995) climatology suggests there are, indeed, many closed density contours over which the constraint can be applied within the upper few hundred meters of the North Atlantic subtropical gyre.
- The potential vorticity is positive definite. This assumption is required for consistency with the neglect of buoyancy forcing. Reversals in sign of the potential vorticity would result in symmetric instability, leading to the fluid column overturning and modifying its density.
- The mean vertical velocity is directed downward within the subtropical gyre. While the vertical velocity is clearly directed downward within the Sverdrup interior, one might speculate that there should be compensating upwelling within the western boundary current. However the meridional streamfunctions from ocean general circulation models do generally reveal surface Ekman cells of the type sketched in Fig. 1 (e.g., Semtner and Chervin 1992), with net downwelling in the subtropical gyre. More directly, Spall (1992) evaluated the three-dimensional trajectories of two fluid parcels within the North Atlantic subtropical gyre of a coarse-resolution numerical model. In both cases Spall found that the fluid parcels described downward spirals as they circulated through the gyre. Here we effectively *impose* a vertical velocity field and explore the consequences for the structure of the thermocline.

Having made these three assumptions, we can now deduce the sign of the area-averaged components of the potential vorticity flux vector, (11)–(13), as shown in Fig. 2.

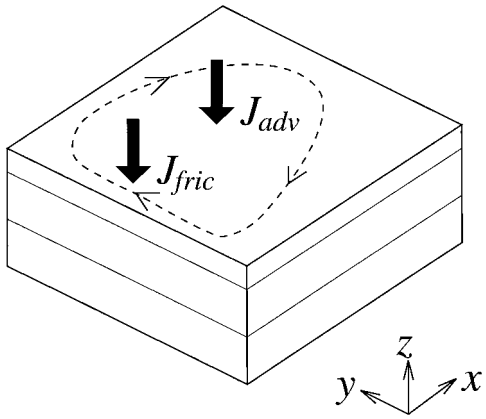

FIG. 2. In an adiabatic subtropical gyre both the advective and frictional components of the vertical potential vorticity flux, J_{adv} and J_{fric}, are directed downward. The dashed line represents a Bernoulli streamline and the light solid lines represent isopycnals. Because the isopycnals are impermeable to the potential vorticity flux vectors, the potential vorticity cannot escape through the base of the gyre, but accumulates in an internal boundary layer thermocline.

Since w is directed downward and Q is positive definite, the *advective* component of the potential vorticity flux, J_{adv}, is directed downward. Having neglected buoyancy forcing, the *buoyancy-forced* component of the potential vorticity flux vanishes by assumption. Finally, in order to determine the sign of the *frictional* component of the potential vorticity flux, we need to consider the cross product of the horizontal density gradient and the frictional force. In a subtropical gyre, density surfaces dome downward implying that the horizontal density gradient is directed outward from the center of the gyre. The frictional force must in general oppose the circulation, and will therefore be directed cyclonically around each streamline. The frictional component of the potential vorticity flux, J_{fric}, is therefore negative, that is, directed downward.

Thus the advective and frictional components both flux potential vorticity downward toward the base of the gyre (Fig. 2). Any potential vorticity initially found at middepths is thus expelled toward the base of the gyre. Because the isopycnals dome downward and are impermeable to the potential vorticity flux vectors, the potential vorticity cannot escape through the base of the gyre, but accumulates within an internal thermocline. In the final steady state, the circulation is confined to a surface layer of uniform density within which the advective and frictional potential vorticity fluxes both vanish independently. The density gradients occur in an infinitely thin internal boundary layer at the base of the gyre.

b. Finite diapycnal diffusion

The completely adiabatic limit leads to a discontinuity in the density field at the base of the gyre. In practice

this discontinuity will be limited by diapycnal mixing, and hence a vertical diffusion of density is now introduced into the analysis,

$$\mathcal{B} = \frac{\partial}{\partial z}\left(\kappa\frac{\partial\rho}{\partial z}\right). \tag{14}$$

The integral balance (10) can now be written

$$\int_A q^{(z)}\left\{-w\frac{\partial\rho}{\partial z} + \frac{\partial}{\partial z}\left(\kappa\frac{\partial\rho}{\partial z}\right) + \frac{F^{(x)}}{q^{(z)}}\frac{\partial\rho}{\partial y} - \frac{F^{(y)}}{q^{(z)}}\frac{\partial\rho}{\partial x}\right\} dx\, dy \approx 0, \tag{15}$$

where the potential vorticity has been approximated by

$$Q \approx -\frac{q^{(z)}}{\rho}\frac{\partial\rho}{\partial z}, \tag{16}$$

consistent with a small Rossby number.

Equation (15) is remarkably similar to the balance between vertical advection and diffusion of density that is assumed to hold *locally* within many similarity thermocline theories (e.g., Salmon 1990), except that here the balance emerges as an *integral constraint* on the structure of the thermocline, and it incorporates an additional term involving frictional forcing.

Assuming a balance between the first two terms in (15), as in the classical similarity thermocline theories, leads to an internal boundary layer thermocline whose thickness scales as

$$\delta \propto \kappa^{1/2} \tag{17}$$

(Stommel and Webster 1962; Young and Ierley 1986; Salmon 1990). As discussed in section 3a, the frictional term should reinforce the advective term, leading to a sharper thermocline than predicted using classical internal boundary layer theory. Indeed the thermocline thicknesses diagnosed in the numerical calculations of Samelson and Vallis (1997) are generally a factor of 2 smaller than those predicted by classical internal boundary layer theory.

c. The two-thermocline limit

The preceding analysis lends support to the internal boundary layer thermocline theory. However the numerical solutions of Samelson and Vallis (1997) contain *both* a surface ventilated thermocline and an internal boundary-layer thermocline.

Consider a fluid column circulating around the subtropical gyre underneath an *imposed* north–south surface temperature gradient. As the column flows equatorward within the Sverdrup interior, ever warmer fluid is pumped down from the surface Ekman layer, creating a strong surface-intensified ''ventilated'' thermocline (Luyten et al. 1983). In contrast as the fluid column returns poleward within the western boundary current, the surface temperature decreases, creating an unstable stratification that must convectively overturn. This scenario was precluded in sections 3a and 3b by setting the surface buoyancy forcing to zero a priori. However we can accommodate convective overturning at the surface by including a mixed layer of variable density and depth in the analysis. As previously, we now consider the sign of the three potential vorticity flux components at different depths within the gyre.

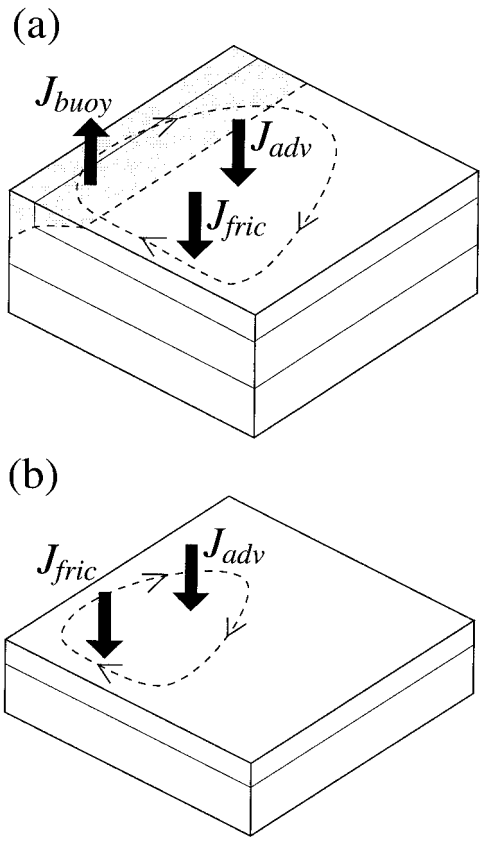

FIG. 3. (a) Within a Bernoulli contour (dashed line) that passes through the surface mixed layer (shaded), the downward advective and frictional potential vorticity fluxes, J_{adv} and J_{fric}, are balanced by an upward potential vorticity, J_{buoy}, provided by buoyancy forcing in the mixed layer. (b) At deeper levels, Bernoulli contours do not pass through the mixed layer. Assuming the net vertical velocity remains downward implies that both the advective and frictional components of the potential vorticity flux are directed downward. Potential vorticity at these depths is again expelled toward the base of the gyre to form an internal thermocline.

First, taking a depth to which the surface mixed layer penetrates, we consider a contour of Bernoulli potential that passes through the mixed layer, Fig. 3a. As in section 3a, the advective and frictional components of the potential vorticity are directed downward. However there is now a third component of the potential vorticity flux associated with buoyancy forcing in the mixed layer. A net cooling is required for the associated potential vorticity flux to be directed upward in order to balance the advective and frictional fluxes. The precise balance will depend on the particular gyre, but it is clear that the integral constraint (10) can be satisfied while main-

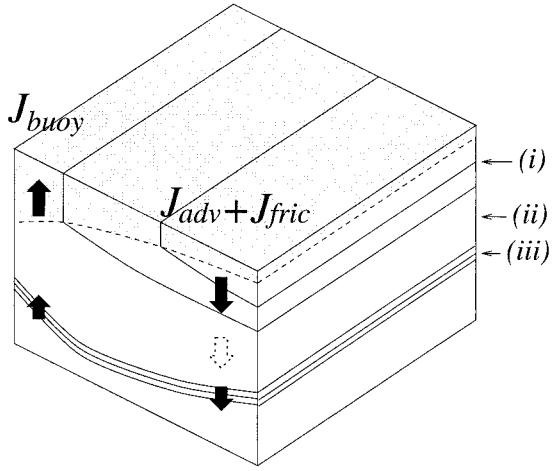

FIG. 4. A summary of the vertical potential vorticity fluxes within a subtropical gyre. (i) *Ventilated regime*: The downward flux of potential vorticity by the advective and frictional components, $J_{adv} + J_{fric}$, is compensated by an upward flux of potential vorticity, J_{buoy}, provided by buoyancy forcing in the mixed layer. (ii) *Mode water regime*: Initially both the advective and frictional components (dotted arrow) flux potential vorticity toward the base of the gyre. Eventually no potential vorticity remains at these depths and the potential vorticity flux vanishes. (iii) *Internal boundary layer regime*: The downward advective and frictional fluxes of potential vorticity across the internal thermocline are balanced by an upward potential vorticity flux provided by density diffusion within the thermocline.

taining a finite potential vorticity (i.e., a ventilated thermocline) at these depths.

But now consider a depth to which surface mixing does not penetrate, Fig. 3b. Assuming that there remains net downwelling at this depth, we return to the previous scenario (section 3a) in which both the advective and frictional components of the potential vorticity flux are directed downward. Any potential vorticity that finds itself at these middepths is once again expelled downward and accumulates within an internal thermocline at the base of the gyre.

In summary, we anticipate three regimes within the gyre (Fig. 4):

1) A *ventilated regime,* where the advective and frictional potential vorticity fluxes are both directed downward and are balanced by an upward flux of potential vorticity provided by buoyancy forcing in the mixed layer.
2) A *mode water regime,* beneath the ventilated thermocline, in which both the advective and frictional components of the potential vorticity flux nearly vanish and the density is nearly uniform.
3) An *internal boundary layer regime,* at the base of the gyre, in which the downward fluxes of potential vorticity associated with advection and friction are balanced by an upward potential vorticity flux associated with diffusion of density across the internal thermocline.

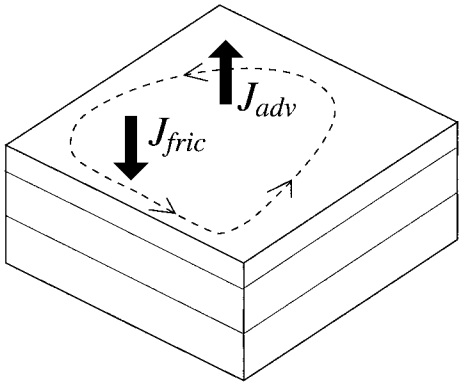

FIG. 5. Within a subpolar gyre, the advective potential vorticity flux, J_{adv}, is upward, but the frictional potential vorticity flux, J_{fric}, is downward. Thus, in contrast to a subtropical gyre, the advective and frictional potential vorticity fluxes can balance without buoyancy forcing.

d. Subpolar gyres

How do these findings translate across to a subpolar gyre (Fig. 5)? In this case we have upwelling and hence the advective flux of potential vorticity is directed upward. However, the same is not true of the frictional potential vorticity flux. Both the horizontal density gradient and the direction of the frictional force are reversed compared with a subtropical gyre. The frictional flux of potential vorticity is therefore directed downward. This result leads to a curious asymmetry between subtropical and subpolar gyres: in a subpolar gyre the advective and frictional potential vorticity fluxes can balance without buoyancy forcing; there is no need for an internal thermocline. A physical explanation for this asymmetry is now developed in section 4.

4. Alternative interpretation as an integral buoyancy budget

Potential vorticity flux vectors provide a general framework for developing integral constraints on the vertical structure of ocean gyres. However, the concept of a potential vorticity flux is somewhat abstract. In this section, an alternative interpretation is developed by rewriting the integral constraint in the form of a buoyancy budget for the Ekman cells connecting adjacent gyres (Fig. 1).

To proceed we need to make two approximations. First, exploiting the fact that the aspect ratio of the ocean is small, the *horizontal* components of the momentum equation, (7), can be approximated by

$$q^{(z)}\mathbf{k} \times \mathbf{u} + \nabla B \approx \mathbf{F}. \tag{18}$$

Second, we approximate the potential vorticity by (16), consistent with the analysis in section 3b. Now rearranging (18) for the horizontal velocity, we obtain

$$\mathbf{u} = \mathbf{u}_B + \mathbf{u}_F, \tag{19}$$

where

$$\mathbf{u}_B = \frac{1}{q^{(z)}}\mathbf{k} \times \nabla B, \tag{20}$$

$$\mathbf{u}_\mathbf{F} = -\frac{1}{q^{(z)}}\mathbf{k} \times \mathbf{F}. \tag{21}$$

Thus we can view the circulation as consisting of two components:

- A *recirculation* of fluid parcels around Bernoulli contours at constant depth, defined by the velocity field ($\mathbf{u}_B$, 0). In a planetary geostrophic limit this simply reduces to the geostrophic velocity.
- A three-dimensional *Ekman circulation,* defined by the velocity field ($\mathbf{u}_\mathbf{F}$, w). This consists a lateral wind-driven Ekman velocity within the surface Ekman layer, downwelling and upwelling within the subtropical and subpolar gyres, and a lateral Ekman velocity across Bernoulli contours associated with frictional forcing.

Using (16) and (21), it is now straightforward to rewrite the integral constraint (10) in the form,

$$\int_A q^{(z)}\left\{\mathbf{u}_\mathbf{F} \cdot \nabla\rho + w\frac{\partial\rho}{\partial z} - \mathcal{B}\right\} dx\, dy \approx 0. \tag{22}$$

Since the absolute vorticity, $q^{(z)}$, should always be positive in the subtropical and subpolar gyres, the constraint (22) can be reinterpreted as an integral buoyancy budget for the three-dimensional Ekman circulation.

For example, consider the passage of a fluid parcel through the Ekman cell connecting the subtropical and subpolar gyres, as sketched in Fig. 6. Starting in the subtropical Ekman layer, the fluid parcel is pumped downward into the subtropical gyre. As it circulates around the subtropical gyre, the fluid parcel both descends and spirals radially outward across Bernoulli contours due to the presence of friction. Eventually, the fluid parcel is transferred across to a Bernoulli contour within the subpolar gyre, where it spirals back up toward the Ekman layer.

As the fluid parcel completes the above circuit, its buoyancy must be modified. Initially the fluid parcel is warm and buoyant as it subducts from the Ekman layer into the subtropical gyre. As the fluid parcel circulates through the subtropical gyre, the Ekman cell requires it to cross the inclined density surfaces and increase its density. However the only source of buoyancy forcing is through the relatively weak density diffusion. The required density transformation can only be achieved if the fluid parcel passes through an internal thermocline where the density gradients, and hence the diapycnal mixing, are enhanced.

Figure 6 also makes clear the cause of the asymmetry between the subtropical and subpolar gyres. In the subtropical gyre, the isopycnals dome downward, and there is no adiabatic pathway between the surface Ekman layer and the subpolar gyre. In contrast in the subpolar gyre, the isopycnals dome upward, and there is an adiabatic pathway back toward the surface Ekman layer. In the subtropical gyre, the Ekman circulation must thus pass through an internal boundary layer thermocline, whereas in the subpolar gyre no internal thermocline is required.

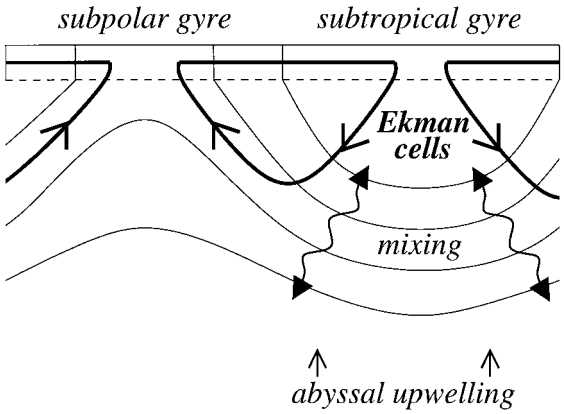

FIG. 6. Schematic diagram demonstrating the physical origin of the internal thermocline at the base of the subtropical gyre. The thick solid lines indicate the Ekman cells, thin solid lines are isopycnals, and the dashed line presents the base of the Ekman layer. In the subtropical gyre, the isopycnals dome downward and the Ekman cells thus take fluid parcels across isopycnals. The necessary buoyancy transformation is provided by diapycnal mixing within the internal thermocline. In the subpolar gyre, the isopycnals dome upward and provide adiabatic pathways along which the Ekman cells can return fluid parcels toward the surface Ekman layer. Note that maintenance of the internal thermocline also requires upwelling of abyssal water from below.

5. Contribution of eddies

Thus far we have assumed that the circulation is steady and free of turbulent eddies. Studies of the circulation in a homogeneous ocean suggest that integral vorticity budgets are significantly modified when transient eddies are included (Marshall 1984). It is therefore important to consider how the constraint on the vertical flux of potential vorticity is modified in the presence of eddies. The inclusion of eddies also suggests some interesting connections between the ideas discussed in this paper and some recent theoretical developments concerning the role of eddies in the Antarctic Circumpolar Current and convective chimneys.

There are several, somewhat complementary, approaches one can take to this problem. Here we choose the formulation of Gent et al. (1995) in which the effect of eddies is represented purely as an adiabatic advection of density by an ''eddy-induced velocity'' or ''bolus velocity,'' $\mathbf{u}^*$. In the interest of mathematical simplicity, we neglect the eddy Reynolds stresses, although the following results are easily generalized to include Reynolds stresses if desired.

We therefore replace the density equation (3) with

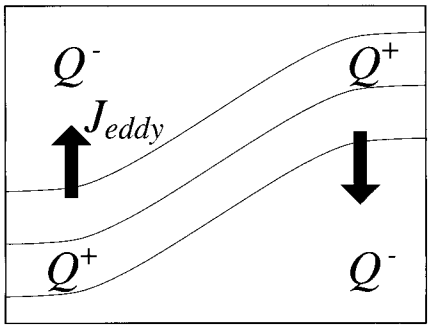

FIG. 7. A schematic diagram illustrating the physical origin of the eddy component of the vertical potential vorticity flux. The figure shows a slumping baroclinic front. Geostrophic eddies act to raise the isopycnals (light solid lines) to the left, fluxing potential vorticity upward; conversely the eddies depress the isopycnals to the right, fluxing potential vorticity downward. Here Q^+ denotes large values of potential vorticity and Q^- denotes small values.

$$(\mathbf{u} + \mathbf{u}^*) \cdot \nabla\rho = \mathcal{B}, \tag{23}$$

where the variables are now reinterpreted as their time-filtered counterparts. The integral constraint, (10), becomes

$$\int_A (J_{\text{adv}} + J_{\text{eddy}} + J_{\text{buoy}} + J_{\text{fric}})\, dx\, dy = 0, \tag{24}$$

where

$$J_{\text{eddy}} = -q^{(z)}\mathbf{u}^* \cdot \nabla\rho \tag{25}$$

is vertical flux of potential vorticity associated with the geostrophic eddies. Note that J_{eddy} involves contributions from *both* the horizontal and vertical components of the bolus velocity.

For a physical interpretation of J_{eddy}, consider the slumping of a baroclinically unstable front, as sketched in Fig. 7. Mimicking the effects of baroclinic instability, the bolus velocity raises the isopycnals to the left of the front and there is an upward flux of potential vorticity. Conversely, to the right of the front, the bolus velocity depresses the isopycnals and there is a downward flux of potential vorticity.

The integral constraint now contains four separate components, making broad conclusions difficult to draw. However, as in section 4, the constraint can be cast in the alternative, more helpful form,

$$\int_A q^{(z)}\left\{(\mathbf{u}_\mathbf{F} + \mathbf{u}_H^*) \cdot \nabla\rho + (w + w^*)\frac{\partial\rho}{\partial z} - \mathcal{B}\right\} dx\, dy \approx 0. \tag{26}$$

Here $\mathbf{u}_H^*$ and w^* represent the horizontal and vertical components of the bolus velocity, respectively. Thus in the presence of eddies, the integral constraint can be interpreted as a buoyancy budget for a net ''secondary circulation,'' $(\mathbf{u}_\mathbf{F} + \mathbf{u}_H^*, w + w^*)$, consisting of both the Ekman circulation and the bolus circulation.

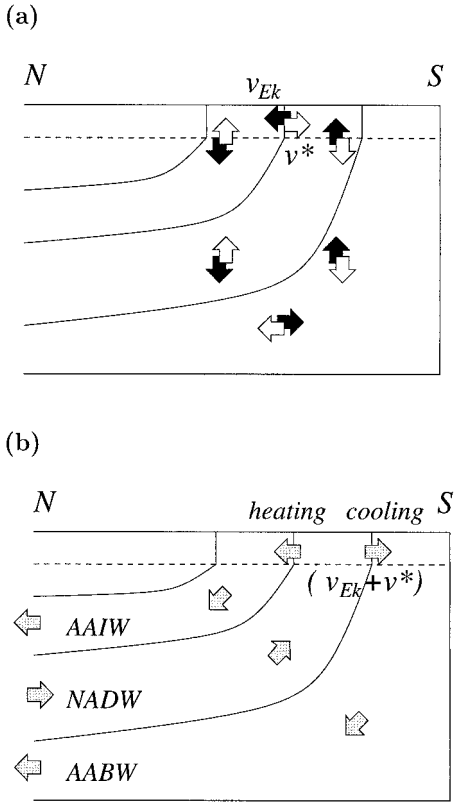

FIG. 8. Schematic diagrams showing the form of the secondary circulation across the ACC in two idealized limits. Solid lines are isopycnals and the dashed line represents the base of the surface Ekman layer. (a) In the limit of no buoyancy forcing, the wind-driven Deacon cell (solid back arrows) is exactly opposed by the bolus velocities (white arrows), such that the net secondary circulation across the ACC vanishes. (b) The prescribed surface heating and cooling drives the net secondary circulation (gray arrows) across isopycnals in the surface Ekman layer. In the interior, the secondary circulation follows the isopycnals, with equatorward transfer of AAIW and AABW, and poleward transport of NADW in between.

a. Antarctic Circumpolar Current

First consider the application of (26) to the Antarctic Circumpolar Current (ACC). The ACC might be considered analogous to subpolar gyres found in the northern hemisphere in as much as the vertical Ekman velocity is upward. The ACC also passes through an equatorward western boundary current—the Malvinas Current—in common with the northern hemisphere subpolar gyres. The interested reader may seek out more detailed discussions of the following points in Marshall (1997).

First consider the hypothetical case of an ACC with no buoyancy forcing, Fig. 8a. The surface winds are westerlies and drive an equatorward Ekman transport. This results in a ''Deacon cell'' that, due the presence of Drake Passage, extends down into the abyssal ocean

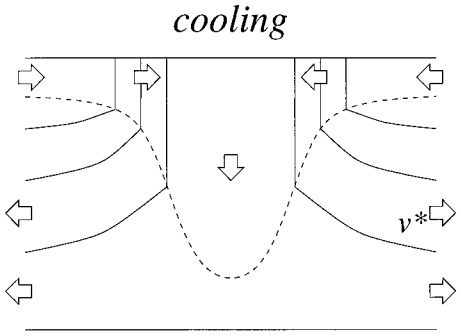

FIG. 9. In a buoyancy-driven gyre, or convective chimney, the Ekman circulation vanishes since there is no mechanical forcing. Thus the bolus velocities converge toward the center of the chimney within the mixed layer and diverge at depth along the sloping isopycnals.

(black arrows).[3] The only way (26) can be satisfied is if the net secondary circulation across the ACC vanishes. Thus the bolus velocities (white arrows) must act to the oppose the Deacon cell. This cancellation of the Deacon cell was first obtained in an ocean general circulation model by Danabasoglu et al. (1994), and is directly analogous to the cancellation of the Ferrel cell in the atmosphere [see, e.g., James (1994)].

But now consider the more realistic scenario in which the buoyancy forcing remains finite within the surface Ekman layer, Fig. 8b. The constraint, (26), now requires the net secondary circulation (shaded arrows) to cross isopycnals within the surface Ekman layer. The particular example shown in Fig. 8b contains a patch of warming over the northern part of the ACC and cooling over the southern part of the ACC. This leads to a transformation of North Atlantic Deep Water (NADW) into both Antarctic Intermediate Water (AAIW) and Antarctic Bottom Water (AABW) within the surface Ekman layer. Within the ocean interior, (26) requires the net secondary circulation to flow along isopycnals with equatorward transport of AAIW and AABW and poleward transport of NADW in between. The circulation pattern in Fig. 8b is broadly in accord with observed tracer distributions. Similar results have also been obtained in numerical simulations, notably by Döös and Webb (1994) and Marsh et al. (2000).

b. Buoyancy-driven gyres

A related application of (26) is to a convective chimney driven by surface buoyancy loss, Fig. 9. In a statistically steady state, the loss of buoyancy through the sea surface is offset by eddies fluxing heat into the chimney from the far field (Legg and Marshall 1993; Visbeck et al. 1996). The zero order flow is along Bernoulli contours, which circle around the chimney.

In contrast to the ACC, the absence of mechanical forcing means that the Ekman circulation vanishes. The integral constraint, (26), thus tells us that the eddy bolus velocities converge toward the center of the chimney within the surface mixed layer and diverge at depth along the sloping isopycnals. (Marshall 1997).

c. Wind-driven gyres

In both the ACC and buoyancy-driven gyres, the structure of the net secondary circulation, including the contribution of eddies, differs at leading order from the Ekman circulation alone. It is natural to wonder whether geostrophic eddies may similarly modify the Ekman cells in the subtropical and subpolar gyres.

It is difficult to resolve this issue without undertaking explicit numerical calculations. Nevertheless it is worth briefly speculating on the robustness of the steady-state thermocline balances to eddies. Returning to Fig. 6, the cause of the internal thermocline can be attributed to the fact that the subtropical Ekman cells pass through the downward doming density surfaces within the subtropical gyre. To avoid the need for an internal thermocline, it is necessary for the eddy bolus velocity to oppose the Ekman cell, as in the idealized ACC solution sketched in Fig. 8a. How likely is such a cancellation to occur?

A series of papers by Bryan (1986, 1991) and Drijfhout (1994) address a closely related issue, the partitioning of the poleward heat transports between mean and eddy components within the subtropical and subpolar gyres. Focusing on the Drijfhout paper, he found a general tendency for the poleward eddy heat transport to compensate for the heat transport carried by the mean flow; indeed at the boundary between the subtropical and subpolar gyres, Drijfhout obtained nearly complete compensation. These results are no more than suggestive in the present context, but the implication is that the bolus circulation may indeed be comparable in magnitude to the mean Ekman cells. If this indeed turns out to be the case, then the thermocline balances discussed in sections 3 and 4 may require substantial revision.

6. Summary and concluding remarks

It has been shown that closing the circulation at the western boundary imposes an integral constraint on the vertical structure of any ocean gyre. In a steady state there can be no net flux of potential vorticity through any closed contour of Bernoulli potential or density. The vertical fluxes of potential vorticity associated with vertical advection, friction, and buoyancy forcing must therefore balance within a closed gyre.

[3] Strictly the return poleward flow at depth is geostrophic. The integral constraint tells us about the secondary circulation across mean Bernoulli contours. Over the upper 3 km, the ACC circuits around Antarctica, so the net secondary circulation across the Bernoulli contours approximates well to the net meridional circulation. At depth, however, the Bernoulli contours are deformed into closed abyssal gyres, and the constraint does not relate directly to the net meridional circulation.

Within a subtropical gyre, the advective and frictional components both flux potential vorticity downward. In a steady state, the compensating upward potential vorticity flux must be provided through buoyancy forcing. Three regimes emerge: a surface ''ventilated thermocline,'' where the upward potential vorticity flux is provided by buoyancy forcing within the surface mixed layer; a ''mode water'' in which all three components of the potential vorticity flux vanish; and an ''internal boundary layer thermocline''at the base of the gyre in which the upward potential vorticity flux is provided by density diffusion. Within a subpolar gyre, the advective and frictional components of the potential vorticity flux are directed upward and downward, respectively, and are able to balance without buoyancy forcing.

Alternatively the integral constraint can be interpreted as providing an integral buoyancy budget for the Ekman cells connecting adjacent gyres. In this context, the internal boundary layer thermocline at the base of the subtropical gyre exists to allow the fluid parcels to cross the downward doming isopycnals within the subtropical gyre. In the subpolar gyre, where the isopycnals dome upward, the Ekman cell can pass adiabatically along the inclined isopycnals.

The formulation has been extended to include a representation of geostrophic eddies through an eddy bolus velocity. The constraint then provides an integral buoyancy budget for the net secondary circulation, including both Ekman and bolus contributions. It remains unclear whether the eddy bolus velocity is likely to significantly alter the structure of the subtropical thermocline. This point clearly requires further investigation.

A corollary of this paper, and also of Samelson and Vallis (1997), is that the formation of mode water is related to the relatively small levels of diapycnal mixing found in the ocean. At first, this appears to contradict the classical view of mode waters forming within deep winter mixed layers (Worthington 1959). However the two mechanisms are, in fact, complementary. Williams (1991) derived a relation between the potential vorticity of subducted water masses and the spatial structure of the winter mixed layer density and depth. In principle, through choosing the mixed layer density and depth to vary appropriately, it is possible to obtain a thermocline in which there is no mode water and the potential vorticity is everywhere finite. In practice, however, winter mixed layers appear to adopt spatial structures that favor the formation of mode waters. This is not coincidental, but a consequence of the gyre dynamics. The integral constraint derived in this paper suggests that the solution containing mode water is that which is dynamically consistent with an assumption of weak diapycnal mixing.

The emphasis in this paper has been on developing a general framework for understanding the vertical structure of oceans gyres. However in order to understand the full implications of this methodology, it will be necessary to undertake a detailed series of investigations using numerical models. Such calculations are in progress and will be reported elsewhere. It is hoped that the vertical fluxes of potential vorticity should prove a rich diagnostic tool for interpreting such models.

Acknowledgments. I am grateful to Steve Belcher, Daniel Jamous, Jochem Marotzke, Michael McIntyre, Jeff Polton, and Ric Williams for comments on a preliminary draft of this manuscript. Financial support was provided by the Natural Environment Research Council, GR3/10157.

REFERENCES

Bryan, K., 1986: Poleward buoyancy transport in the ocean and mesoscale eddies. *J. Phys. Oceanogr.,* **16,** 927–933.

——, 1991: Poleward heat transport in the ocean. *Tellus,* **43,** 104–115.

Danabasoglu, G., P. R. Gent, and J. C. McWilliams, 1994: The role of mesoscale tracer transports in the global ocean circulation. *Science,* **264,** 1123–1126.

Döös, K., and D. J. Webb, 1994: The Deacon Cell and the other meridional cells of the Southern Ocean. *J. Phys. Oceanogr.,* **24,** 429–442.

Drijfhout, S., 1994: Heat transport by mesoscale eddies in an ocean circulation model. *J. Phys. Oceanogr.,* **24,** 353–369.

Gent, P. R., J. Willebrand, T. J. McDougall, and J. C. McWilliams, 1995: Parameterizing the eddy-induced tracer transports in ocean circulation models. *J. Phys. Oceanogr.,* **25,** 463–474.

Haynes, P. H., and M. E. McIntyre, 1987: On the evolution of vorticity and potential vorticity in the presence of diabatic heating or other forces. *J. Atmos. Sci.,* **44,** 828–841.

——, and ——, 1990: On the conservation and impermeability theorems for potential vorticity. *J. Atmos. Sci.,* **47,** 2021–2031.

James, I. N., 1994: *Introduction to Circulating Atmospheres.* Cambridge University Press, 422 pp.

Legg, S. A., and J. C. Marshall, 1993: A heton model of the spreading phase of open-ocean deep convection. *J. Phys. Oceanogr.,* **23,** 1040–1056.

Lozier, M. S., W. B. Owens, and R. G. Curry, 1995: The climatology of the North Atlantic. *Progress in Oceanography,* Vol. 36, Pergamon, 1–44.

Luyten, J. R., J. Pedlosky, and H. Stommel, 1983: The ventilated thermocline. *J. Phys. Oceanogr.,* **13,** 292–309.

Marsh, R., A. J. G. Nurser, A. P. Megann, and A. L. New, 2000: Water mass transformation in the Southern Ocean of a global isopycnal coordinate GCM. *J. Phys. Oceanogr.,* **30,** 1013–1045.

Marshall, D. P., 1997: Subduction of water masses in an eddying ocean. *J. Mar. Res.,* **55,** 201–222.

Marshall, J. C., 1984: Eddy-mean flow interaction in a barotropic ocean model. *Quart. J. Roy. Meteor. Soc.,* **110,** 573–590.

——, and A. J. G. Nurser, 1992: Fluid dynamics of oceanic thermocline ventilation. *J. Phys. Oceanogr.,* **22,** 583–595.

——, D. Jamous, and J. Nilsson, 2000: Entry, flux, and exit of potential vorticity in ocean circulation. *J. Phys. Oceanogr.,* in press.

McCartney, M. S., 1982: The subtropical recirculation of mode waters. *J. Mar. Res.,* **40** (Suppl.), 427–464.

McIntyre, M. E., and W. A. Norton, 1990: Dissipative wave-mean interactions and the transport of vorticity or potential vorticity. *J. Fluid Mech.,* **212,** 403–435.

Niiler, P. P., 1966: On the theory of wind-driven ocean circulation. *Deep-Sea Res.,* **13,** 597–606.

Obukhov, A. M., 1962: On the dynamics of a stratified fluid. *Dokl. Akad. Nauk SSSR,* **146** (6), 1239–1242. [English *Sov. Phys. Dokl.,* **7,** 682–684.]

Pedlosky, J., 1996: *Ocean Circulation Theory.* Springer Verlag, 453 pp.

Robinson, A. R., and H. Stommel, 1959: The oceanic thermocline and associated thermohaline circulation. *Tellus,* **11,** 295–308.

Salmon, R., 1990: The thermocline as an internal boundary layer. *J. Mar. Res.,* **48,** 437–469.

Samelson, R. M., and G. K. Vallis, 1997: Large-scale circulation with small diapycnal diffusion: The two-thermocline limit. *J. Mar. Res.,* **55,** 223–275.

Schär, C., 1993: A generalization of Bernoulli's theorem. *J. Atmos. Sci.,* **50,** 1437–1443.

Semtner, A. J., and R. M. Chervin, 1992: Ocean general circulation from a global eddy-resolving model. *J. Geophys. Res.,* **97,** 5493–5550.

Spall, M. A., 1992: Cooling spirals and recirculation in the subtropical gyre. *J. Phys. Oceanogr.,* **22,** 564–571.

Stommel, H., and J. Webster, 1962: Some properties of thermocline equations in a subtropical gyre. *J. Mar. Res.,* **20,** 42–56.

Sverdrup, H. U., 1947: Wind-driven currents in a baroclinic ocean; with application to the equatorial currents of the eastern Pacific. *Proc. Natl. Acad. Sci.,* **33,** 318–326.

Truesdell, C., 1951: Proof that Ertel's vorticity theorem holds in average for any medium suffering no tangential acceleration on the boundary. *Geofis. Pura Appl.,* **19,** 167–169.

Visbeck, M., J. C. Marshall, and H. Jones, 1996: Dynamics of isolated convective regions in the ocean. *J. Phys. Oceanogr.,* **26,** 1721–1734.

Welander, P., 1959: An advective model of the ocean thermocline. *Tellus,* **11,** 309–318.

——, 1971: Some exact solutions to the equations describing an ideal-fluid thermocline. *J. Mar. Res.,* **21,** 60–68.

Williams, R. G., 1991: The role of the mixed layer in setting the potential vorticity of the ventilated thermocline. *J. Phys. Oceanogr.,* **21,** 1803–1814.

Worthington, L. V., 1959: The 18° water in the Sargasso Sea. *Deep-Sea Res.,* **5,** 297–305.

Young, W. R., and G. R. Ierley, 1986: Eastern boundary conditions and weak solutions of the ideal thermocline equations. *J. Phys. Oceaogr.,* **16,** 1884–1900.